EUROFUSION WPJET1-CP(16) 15005

M Goniche et al.

Ion Cyclotron Resonance Heating for tungsten control in various JET H-mode scenarios

Preprint of Paper to be submitted for publication in
Proceedings of 26th IAEA Fusion Energy Conference

This work has been carried out within the framework of the EUROfusion Consortium and has received funding from the Euratom research and training programme 2014-2018 under grant agreement No 633053. The views and opinions expressed herein do not necessarily reflect those of the European Commission.

Ion Cyclotron Resonance Heating for tungsten control in JET H-mode scenarios

M.Goniche[1], R.J.Dumont[1], V.Bobkov[2], P.Buratti[3], S.Brezinsek[4], C.Challis[5], L.Colas[1], A.Czarnecka[6], P.Drewelow[2], N.Fedorczak[1], J.Garcia[1], C.Giroud[5], M.Graham[5], J.P.Graves[7] , J.Hobirk[2], P.Jacquet[5], E.Lerche[8], P.Mantica[9], I.Monakhov[5], P.Monier-Garbet[1], M.F.F. Nave[10], C.Noble[5], I.Nunes[10], T.Pütterich[2], F.Rimini[5], M.Sertoli[2], M.Valisa[11] , D. Van Eester[8] and JET Contributors*

EUROfusion Consortium, JET, Culham Science Centre, Abingdon, OX14 3DB, UK
[1]CEA, IRFM, F-13108 Saint-Paul-lez-Durance, France.
[2]Max-Planck-Institut für Plasmaphysik, Boltzmannstr. 2, 85748 Garching, Germany
[3]ENEA, C.R. Frascati, Via E. Fermi 45 00044 Frascati (RM), Italy
[4]Forschungszentrum Jülich GmbH, 52425 Jülich, Germany
[5]CCFE, Culham Science Centre, Abingdon, OX14 3DB, UK.
[6]IPPLM, Hery 23, 01-497 Warsaw, Poland
[7]Ecole Polytechnique Fédérale de Lausanne (EPFL), 1015 Lausanne, Switzerland
[8]1LPP-ERM/KMS, EUROfusion Consortium Member - Trilateral Euregio Cluster, Brussels, Belgium
[9]Istituto di Fisica del Plasma 'P.Caldirola', Consiglio Nazionale delle Ricerche, Milano, Italy
[10]Instituto de Plasmas e Fusão Nuclear, IST, Universidade de Lisboa, Portugal
[11]Consorzio RFX, Consiglio Nazionale delle Ricerche, Padova, Italy
** See the author list of 'Overview of the JET results in support to ITER' by X. Litaudon et al. to be published in Nuclear Fusion Special issue: overview and summary reports from the 26th Fusion Energy Conference (Kyoto, Japan, 17-22 October 2016*

e-mail contact of main author: marc.goniche@cea.fr

Abstract. Ion Cyclotron Resonance Heating (ICRH) in the hydrogen minority scheme provides central ion heating and acts favorably on the core tungsten transport. Full wave modeling shows that, at medium power level (4MW), after collisional redistribution, the ratio of power transferred to the electrons in the core (r/a<0.25) decreases by ~40% when the minority (hydrogen) concentration n_H/n_e increases from 3% to 10%. At the same time, the high-Z impurity screening provided by the fast ions temperature increases by a factor ~2.
The power radiated by tungsten in the core of the JET H-mode discharges has been analyzed on a large database covering the 2013-2014 campaign. In the baseline scenario with moderate plasma current (I_p=2.5MA) ICRH modifies efficiently tungsten transport to avoid its accumulation in the plasma centre and, when the ICRH power is increased, the tungsten radiation peaking evolves as predicted by the neo-classical theory. At higher current (3-4MA), tungsten accumulation can be only avoided with 5MW of ICRH power with high gas injection rate. For discharges in the hybrid scenario, the strong initial peaking of the density leads to strong tungsten accumulation.. MHD activity plays a key role in tungsten transport and modulation of the tungsten radiation during a sawtooth cycle is often correlated to the fishbone activity triggered by the fast ion pressure gradient.

1. Introduction

In order to prepare the ITER plasma scenarios, the divertor and first wall of the JET tokamak has been changed in 2011. The main chamber plasma facing components are made of beryllium, and the divertor is made of either plain tungsten tiles or tungsten-coated tiles (ITER-like wall, ILW). Tungsten like all high Z atoms, has a very high radiation capability which leads to a detrimental effect on plasma performance if this impurity concentration in the core is too high. Neoclassical theory predicts an inward pinch leading to an accumulation of high Z impurities in the very core of the plasma (r/a<0.2). Moreover, strong plasma rotation occurs in neutral beam heated plasmas and the resulting centrifugal force is the cause of poloidal asymmetry enhancing the radiation on the low field side of the plasma [1,2].

This deleterious effect is mitigated by temperature screening and the sign of convection can be reversed when the ion temperature gradient is sufficiently large with respect of the ion density gradient. Under some assumptions [1,2], when the poloidal asymmetries are not considered the tungsten flux can be expressed as
$\Gamma w \sim n_i T_i \nu_{iW} Z_W (R/L_{ni} - 0.5R/L_{Ti}) \sim n_i T_i^{-1/2} Z_W (R/L_{ni} - 0.5R/L_{Ti})$
where L_X is the inverse of the logarithmic gradient d[log(X)]/dR. However these poloidal asymmetries, arising from the centrifugal force, are important for heavy impurities and an additional term with a positive sign (inward flux) has to be added to Γw.
Ion cyclotron resonance heating (ICRH) can beneficially affect the tungsten transport for several reasons. Firstly a large part of wave energy can be transferred to the bulk ions either by Coulomb collisions with the fast minority ions or by direct damping on the majority ions [3,4]. Secondly, the fast ion tail, characterized by a temperature T_f, can contribute to the impurity screening [2] as the screening scales as $n_f T_f^{-1/2} (R/L_{Tf})$ and very local deposition of ICRH leads to normalized gradient R/L_{Tf} which can exceed 5. Thirdly, the poloidal asymmetry of tungsten radiation, due to the centrifugal force in strongly rotating plasmas with NBI heating, is reduced by the temperature anisotropy of the minority species [5]. In addition to the neo-classical effects, turbulent transport can be enhanced by core electron heating provided by ICRH waves. Finally, MHD activity and particularly core (1,1) modes can allow a flushing of the tungsten from the core of the discharge [6].
The drawback of using ICRH in metallic environment is related to enhanced high Z material sputtering arising from ions accelerated by the DC rectified potential [7, 8]. Therefore the main issue when using ICRH is whether or not the beneficial effect on high Z impurities transport overcomes the detrimental increase of the tungsten source.
In this paper, tungsten radiation from ICRH-heated plasmas ($P_{ICRH} \leq 6$MW) is analyzed on a large database covering the JET baseline scenario with plasma current in the 2.5-4MA range (Bt=2.7-3.8T) and the hybrid scenario at 2.5MA (Bt~2.9T).
Radiation and concentration of tungsten in the core of the discharge are derived from the soft X-ray (SXR) diagnostic, providing a poloidal map of these quantities [9]. For the calculation of the radiated power and tungsten concentration, it is assumed that all the radiation is only from tungsten. From the poloidal asymmetry of the SXR radiation, the toroidal rotation was calculated and compared to the measurements from the charge exchange spectroscopy diagnostic. A very good agreement was found for discharges performed from the beginning to the end of the 2014 campaign and we conclude that lighter metal impurities (Mo and Ni) do not contribute significantly to the SXR radiation in the plasma core (r/a<0.5). As a rule of thumb a power volume density of 0.1MW/m^3 corresponds to a tungsten concentration of 10^{-4} which is usually considered as the upper limit to maintain high performance. In the following of this paper we define the tungsten peaking factor is defined as the ratio of the flux surface-averaged radiation power densities $PF_{0.3} = P_{rad}\text{-W(r/a=0)} / P_{rad}\text{-W(r/a=0.3)}$.
The ion temperature in the very core of the discharge (r/a<0.3) is not measured for the discharges analyzed here and the following proxy will be used for the tungsten flux in the core $\Gamma w \sim R/L_{ne} - 0.5R/L_{Te}$ that is to say $n_i = k_n n_e$ and $T_i = k_T T_e$.

2. Modelling of the ICRH damping and temperature screening by the fast ions

In order to investigate the mechanism of ICRH power deposition when the hydrogen minority concentration n_H/n_e is varied, the EVE/AQL code [4] was run for a high power discharge (P_{NBI}=24MW, P_{ICRH}=4MW) with n_H/n_e varying between 0.25% and 15% while keeping the electron and bulk ion temperature profile identical ($T_e(0)$=7.5keV and $T_i(0)$=7.5 keV). When the minority concentration is increased, wave energy is transferred from the deuterium

(majority 2nd harmonic heating scheme) to the hydrogen (minority 1st harmonic heating scheme) whereas the fraction damped directly on the electrons does not vary much. The fast ion tail does not extend beyond the normalized radius r/a=0.35 and the hydrogen temperature out of this limit is the temperature of the background ions. The temperature anisotropy $T_{perp}/T_{//}$ also decreases from 4.5 at low concentration (n_H/n_e=1%) to 1.2 at high concentration (n_H/n_e=15%).

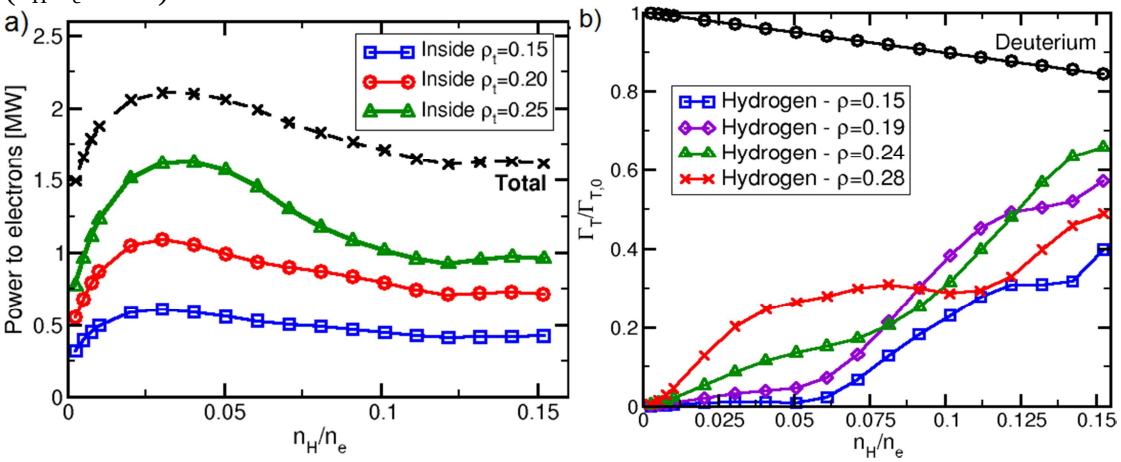

FIG. 1 a) Fraction of RF power transferred to the electrons and ions after collisional redistribution. P_{NBI}=24MW, P_{ICRH}=4MW. b) Temperature screening factor Γ_T normalized to the case of a pure D plasma $\Gamma_{T,0}$ for fast H and thermal D ions.

Collisional redistribution of the absorbed power to the D ions increases when n_H/n_e increases from 4% to 12% and then levels off for larger concentration. This mostly results from the increasing thermal contribution to the total hydrogen ion energy as the minority concentration increases. As a consequence, the total power absorbed by the electrons in the core plasma (r/a<0.25) decreases from 1.6MW (40% of the total power) to 1.0MW (25% of the total power) when the H concentration is increased from 3% to 10% (Figure 1a). Experiments carried out with hydrogen minority concentration varying between 2% and 23% [10, 11] show that when n_H/ne is increased from 2% to 15%, the central electron temperature decreases by 20% when the ion temperature, deduced from the neutrons rate, decreases by only 12%, indicating a relative increase of the power damped on the deuterium ions at high H concentration but this power does not increase with this concentration as a result of weaker absorption of the wave. In the experiments, the power fraction going to the electrons is significantly more important than expected from modelling at low concentration (n_H/n_e=2-3%). This could be the result of the additional electron heating provided by the fast deuterium population which is not taken into account in this modelling. The observed slight increase of W peaking when the minority concentration is increased is therefore qualitatively correlated to the decrease of electron and ion temperatures.

From the modelled fast ion temperature profile, the temperature screening factor $n_f T_f^{-1/2}(R/L_{Tf})$ was computed and compared to the temperature screening factor provided by the thermal deuterium ions. This screening factor is found to be the highest at r/a~0.28 for the low range of hydrogen concentration (3%<n_H/n_e<10%) and the maximum moves inwards for higher concentrations (figure 1-b). For the usual cases of ICRH with n_H/ne <10%, the screening provided by the fast H ions is much lower (at least a factor 3) than that provided by the thermal D ions. The screening by fast ions and thermal ions, with n_H/ne=9%, was found of the same order in a previous work [2]. Taking into account, the large uncertainty on the temperature gradient dT_f/dR for the calculation of the screening factor, the screening factor

has an error bar of at least ±30% but surely this factor increases with n_H/ne although the temperature of the fast ions sharply decreases. However, experimentally the peaking of tungsten concentration is observed to be the lowest for n_H/n_e~2% when the screening factor by the fast ions is the lowest and we conclude that screening of W by the ICRH fast ions plays a minor role in these experiments.

3. ICRH in JET Baseline scenario

3.1 Medium plasma current experiments

ICRH power varying between 0 and 6MW was coupled to 2.7T/2.5MA discharges with total power close to 20MW at a frequency of 42.5MHz providing central heating with the IC resonance layer located about 5cm from the magnetic axis on the high field side in most cases. The first series was performed with the outer strike point on the tile 5 of the bottom divertor (R_{OSP}~2.73m) and gas rate in the range of 0.9-1.2×10^{22} el./s . This allows to be well above the L-H transition and to get type I ELMs with frequencies in the 30-45 Hz range. For the same total power (19-20MW), when the ICRH power is increased from 0 to 6MW, a strong decrease of the tungsten radiation in the very core (r/a~0) from 0.2MW/m^3 to 0.07MW/m^3 is observed and the W radiation peaking decreases correspondingly from ~10 to ~1.6.(Fig. 2-a).

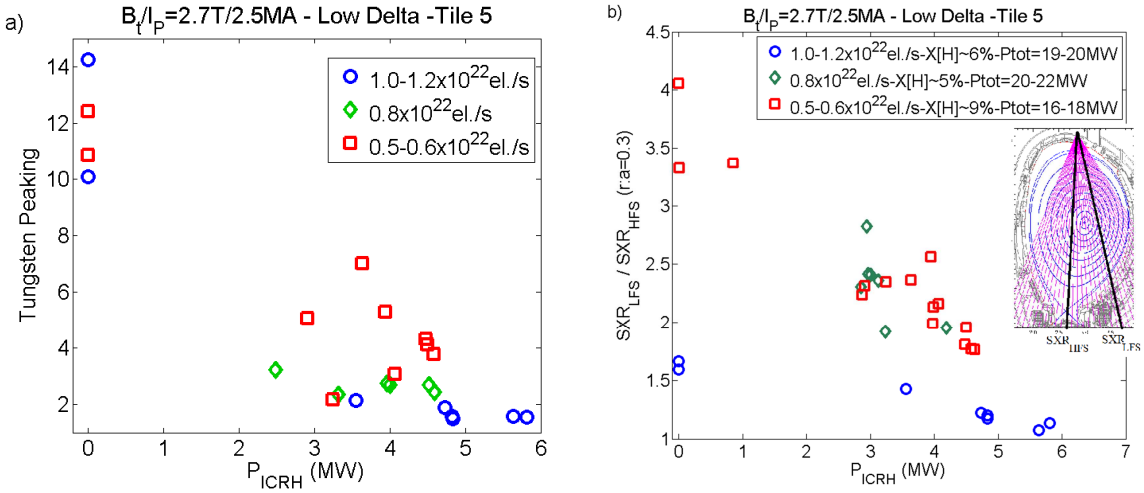

FIG. 2 a) Tungsten peaking. b) Asymmetry of the SXR radiation in the mid-plane at r/a=0.3. Data collected at least 2seconds after the start of the high power phase

The LFS/HFS asymmetry of the SXR radiation can be estimated from the ratio of the raw signals given by the lines of sight tangent to the same magnetic surface (r/a=0.3) (Fig. 2-b). This asymmetry decreases from 3.5-4 (P_{ICRH}=0) to 1.8 (P_{ICRH}~4.5MW) for the low gas rate case. This effect could the result of the reduced toroidal rotation when adding ICRH (the NBI power is reduced by 20-30% to keep the total power constant) but the impact of ICRH on the asymmetry is too strong to be only caused by the change of toroidal rotation and the stronger temperature anisotropy of the hydrogen when the ICRH is increased is also the cause of reduced radiation asymmetry. As an effect of the reduced contamination of the plasma core by high-Z impurities, the energy confinement, evaluated from the $H_{98y,2}$ factor, slightly increases from ~0.72 to ~0.77, when correction for the ICRH fast ion contribution to the plasma diamagnetic energy was applied. At low gas rate (~0.5×10^{22} el./s), the ELM frequency decreases to 15-20Hz and the core tungsten radiation increases strongly. However the SXR radiation asymmetry decreases linearly with power from ~4 (P_{ICRH}=0) to ~1.8 (P_{ICRH}=4.6MW). When the outer strike point is moved closer to the pumping duct

(R_{OSP}~2.92m), with higher gas dosing (1.7×10^{22} el./s), high ELM frequency (~100Hz) is combined with low radiation (P_{rad}/P_{tot}~20%, P_{rad}-W(0)~0.06MW/m^3) and similar confinement ($H_{98,y}$~0.85) to that of the low gas dosing case with low pumping (R_{OSP}~2.75m) is obtained.
For all gas dosing and pumping cases, the normalized logarithmic gradient of the electron temperature R $(dT_e/dR)/T_e=R/L_{Te}$, increases from ~2 to ~5 when the ICRH power increases from 0 to 6MW). The equivalent quantity for the density, R/L_n, decreases with the ICRH power from ~1.5 to ~0.5 for the low pumping case. In the case of high pumping and high gas dosing, the central density is significantly lower ($n_e(0)$~6×10^{19} m^{-3}) compared to the low pumping case ($n_e(0)$~7×10^{19} m^{-3}) with 4MW of ICRH power and the normalized logarithmic gradient is higher (R/L_n~2).
The tungsten radiation peaking was estimated for a large data base including pulses with various P_{tot} (15-20MW), P_{ICRH} (0-6MW), minority hydrogen concentration X[H] (2-20%). A good correlation between $R/L_{ne} - 0.5R/L_{Te}$ and the tungsten peaking which is varying between 1 and 14 (Fig. 3) is found. The beneficial effect of ICRH on the gradients is clearly observed and the sign of convection is inverted from inward to outward for an ICRH power exceeding 3MW for most cases.
However, a significant difference is observed between low gas rate/low pumping pulses (+ symbols of Fig. 3) and high gas rate/high pumping pulses (× symbols): although they have almost the same $R/L_{ne} - 0.5R/L_{Te}$ value, higher peaking of the tungsten radiation is observed for the low gas rate pulses. In that case we may expect a net higher tungsten influx from the edge resulting from the lower ELM frequency [12] but also possibly from the higher RF rectified sheath, caused by the higher antenna electric field (the antenna coupling resistance is lower by 20-25% in this case) [13, 14]. Consistently, the core tungsten radiation is about 10 times higher when compared to the high gas rate cases.

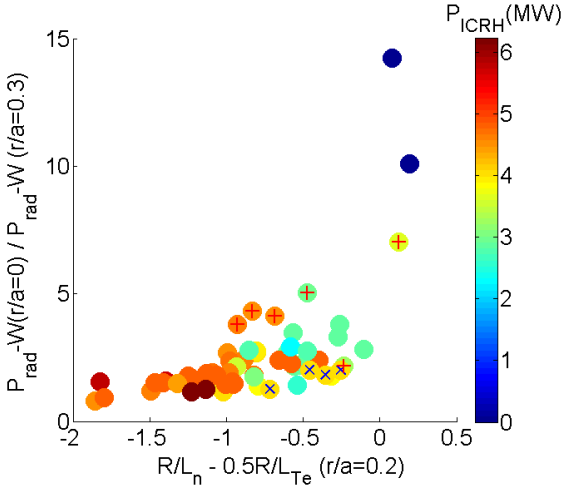

FIG.3. Tungsten radiation peaking (from SXR measurements) as a function of $R/L_{ne} - 0.5R/L_{Te}$.. Low gas rate/low pumping (+) and high gas rate/high pumping (×) cases are highlighted

3.2 High Plasma current experiments
During the recent development of the baseline scenario, in preparation of the D-T campaign, the plasma current was increased from 2.5 to 4.0MA while keeping q_{95} close to 3 (B_t=2.7-3.7T) [15]. The outer strike point was close to the pumping duct (R_{OSP}~2.92m) and the gas injection rate was increased with respect of the lower plasma experiments ($2\text{-}5\times10^{22}$ el./s). The total power was varied between 15MW and 30MW and the ICRH power was in the 2-5MW range. The position of the IC resonance layer is constrained by the scenario and the available bands of frequency of the ICRH generators. As a consequence the position of the IC resonance layer was varied such as $0<R_{IC}-R_{mag}<0.40$m.
At 3.0MA with medium gas injection (~3×10^{22} el./s), leading to a high ELM frequency (~100Hz), the maximum core tungsten peaking increases regularly from one sawtooth cycle to the next one (figure 11-a), exceeding 4, 3 seconds after the start of the ICRH power (P_{ICRH}=4.5MW). The W radiation peaking reaches a maximum ~200ms before the sawtooth

crash and then decays, this change in character coinciding with a change in MHD activity [16]. The peaking phase is accompanied by two independent (1,1) modes: low amplitude, fast-cycling (< 5 ms) fishbones (chirping in frequency range 11-17 kHz) and a lower frequency (~9 kHz) bursting (1,1) mode. In the second phase when the radiation profile flattens, the lower frequency, bursting mode has disappeared, while the fishbones have gained strength and their cycles are much slower (> 10ms).

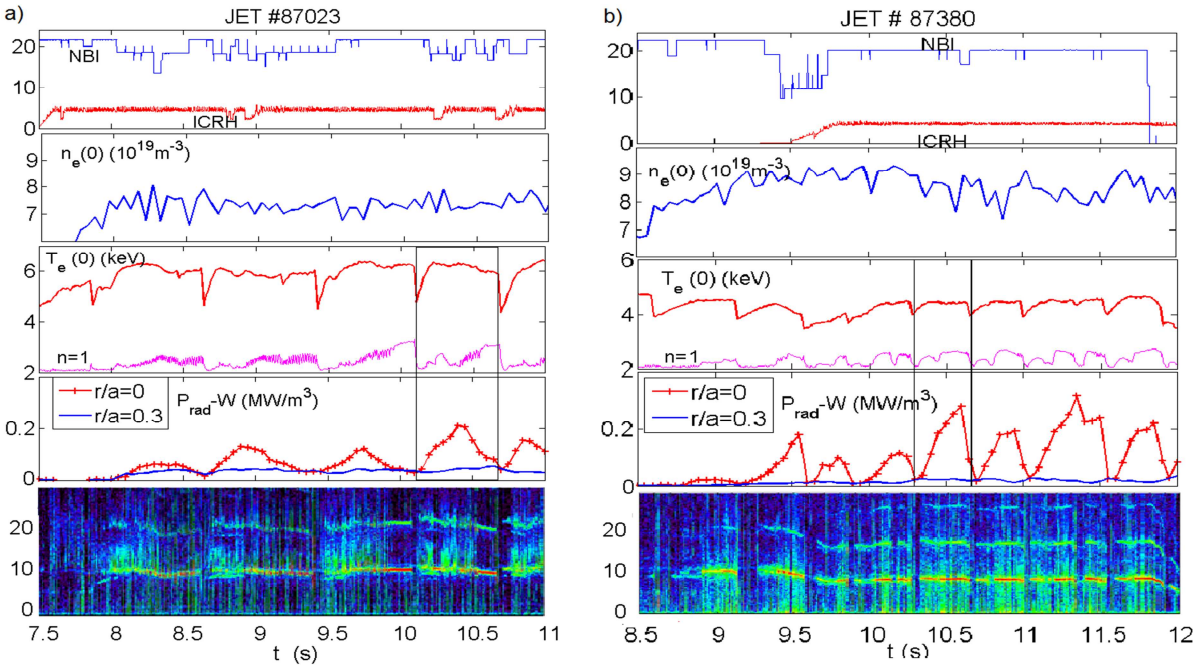

FIG. 4. Time traces of 3MA/2.9T discharge a) R_{IC}-R_{mag}=0.10m, X[H] ≈5%) b) R_{IC}-R_{mag}=0.39m, X[H] ≈7%.

When the IC resonance is moved out of the q=1 surface (R_{IC}-R_{mag} =0.39m), although the gas rate is strongly increased (~5×10^{22} el./s) and maintaining the same ELM frequency (~100Hz), peaking of the tungsten radiation increases to very high values (10-20) until the sawtooth crashes (Fig.4-b). No fishbone activity is detected in that case. For these two discharges the $R/L_{ne} - 0.5R/L_{Te}$ parameter is lower for central heating (~-1) than for the off-axis heating (~0) when the average tungsten peaking, averaged over 1s, varies between 2 and 3 for the first case and 6 and 7 for the second one. These data (peaking vs $R/L_{ne} - 0.5R/L_{Te}$) fit those obtained at 2.5MA with low gas rate /low pumping (+ symbols of Fig.3).

When the current is further increased to 3.5MA with quite low gas injection (~2×10^{22} el./s) and low ELM frequency (~40Hz), the maximum tungsten peaking increases during the 3-second high power phase up to ~10. The maximum of W radiation peaking is now observed only ~100ms after the sawtooth crash (t_{ST}~600ms) with central hating. The $R/L_{ne} - 0.5R/L_{Te}$ quantity is unchanged (~-1). This is roughly consistent with the W radiation peaking, which increases only from ~2 (2.5MA) to ~3 (3MA), 1.5s after the start of the ICRH power. Beneficial effect of ICRH above 3-4MW on tungsten peaking is confirmed (Fig.5). However, at moderate gas injection (1-2×10^{22} el./s, closed symbols), there is a significant increase of the tungsten peaking at high plasma current (I_p=3.0-4.0MA) with respect of the peaking obtained at lower current (I_p=2.5MA).

A rather flat tungsten profile (peaking ~1.5) can be achieved at 3-3.5MA with high ICRH power (P_{ICRH}~5MW) and high gas rate (~3×10^{22} el./s at 3MA, ~4×10^{22} el./s at 3.5MA, open

symbols) at the expense of the global energy confinement (H_{98y}~0.75) of these low triangularity plasmas.

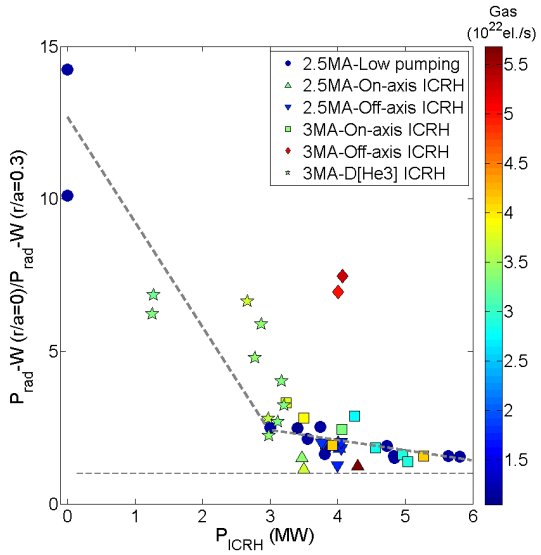

FIG. 5. Tungsten radiation peaking versus ICRH powers. Data, averaged on 1s, are taken 2s after the start of the high power phase.

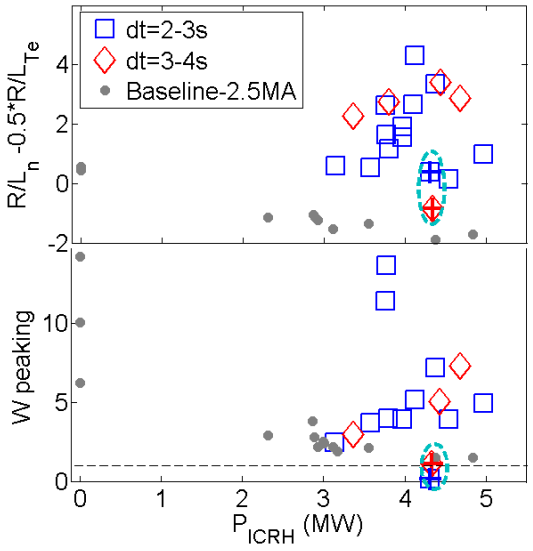

FIG. 6. Normalized gradients and Tungsten radiation peaking for two time slices dt after the start of the high power phase.

4. ICRH in JET Hybrid scenario

Experiments with the hybrid scenario (flat q profile with q_0~1) were conducted on JET with the ILW at I_p=2.5MA and B_t=2.9T [17]. This scenario allows ICRH in the hydrogen minority heating scheme with R_{res}-R_{magn}=0.08-0.20m (LFS), depending on the normalized plasma pressure. In the reported experiments, the total power is in the 22-27MW range, the ICRH power in the 2.8-5.0MW range. The gas injection rate (0.9-1.5×10^{22}el./s) is reduced with respect of the baseline scenario aiming at achieving high confinement regime (H_{98y}>1). The hybrid scenario is characterized by a more peaked density profile the baseline scenario. This is the generally the result of the lower collisionality of these plasmas [18, 17]. In order to get the required q-profile, the high power phase is generally started earlier in the discharge, typically at t=5.5s for NBI and ICRH when NBI (resp. ICRH) is started at t=7.s (resp.7.5s) in the case of the baseline scenario. For these discharges, the normalized density gradient R/L_n, measured 1s after the start of the high power phase varies between 2 and 3 when it is in the 1-1.5 range for 3.0-3.5MA baseline discharges in the same range of total injected power (20-26MW).

When the NBI and ICRH powers are applied, the density starts peaking 2-2.5s after the start of this high power phase and tungsten accumulates in the plasma core. The central temperature decreases but the normalized T_e gradient is sometimes maintained high (R/L_{Te}>4). The resulting R/L_n – 0.5R/L_{Te} parameter is positive (Fig.6). No beneficial effect of the ICRH power between 3and 5MW on the core radiation (r/a<0.3) is observed. Although scans of IC resonance position have shown weak (but beneficial) effect of this parameter when the resonance is moved away on the LFS from the magnetic center on the tungsten radiation peaking, there is still an uncertainty on the effect of very central ICRH (r/a<0.1) in the hybrid scenario.

In one case, when the start of the high power phase was delayed by 0.5s (t_{start}=6s) and slightly more injected gas (1.3×10^{22}el./s), the low initial density peaking is maintained and even

decreases during the high power phase (R/L_n decreases from 1.6 to 0.7). For this discharge, the tungsten radiation profile is maintained hollow with very low radiation in the core (<0.02MW/m^3 at r/a=0) for 3s. A similar discharge with earlier timing has a strong 3/2 mode. This NTM is a strong player in accelerating the impurity accumulation as previously observed [6]. However, the good confinement of the low tungsten core radiation discharge (H_{98y}~1.1, β_N~1.9) is not sustained beyond t- t_{start} =3s as the current profile evolves and the first sawtooth is triggered at t- t_{start}=2.5s.

5. Conclusions.

Modelling of Ion Cyclotron Resonance Heating in the hydrogen minority scheme indicates that the ion heating of the plasma core (r/a<0.25) increases significantly (+50%) when the hydrogen concentration increases to the 10-15% range and, at the same time, the temperature screening from fast ions increases. However these beneficial effects of high n_H/ne are very likely impeded by the weaker absorption of the wave at high concentration.

Central ICRH in the 4-6 MW range has clearly beneficial effect on tungsten transport in the baseline scenario, but at high plasma current higher ICRH power is required to access to very low W peaking factor ($PF_{0.3}$<1.5). In the hybrid scenario, although very low W concentration in the core has been achieved in a unique pulse for 3s, the efficiency of higher power (7-8MW) for avoiding tungsten accumulation is still questionable.

Acknowledgements

This work has been carried out within the framework of the EUROfusion Consortium and has received funding from the EURATOM research and training programme 2014-2018 under grant agreement No 633053. The views and opinions expressed herein do not necessarily reflect those of the European Commission.

References

[1] ANGIONI C. et al., Nucl. Fusion 54 (2014) 083028 (26pp)
[2] CASSON F. Plasma Phys. Control. Fusion 57 (2015) 014031 (10pp)
[3] MANTSINEN.M. et al , Plasma Phys. Control. Fusion 41 (1999) 843–865
[4] DUMONT R.J. and ZARZOSO D., 2013 Nucl. Fusion 53 013002 [
[5] BILATO R. et al., Nucl. Fusion 54 (2014) 072003 (4pp)
[6] HENDER T.C. et al, Nucl. Fusion 56 (2016) 066002 (15pp)
[7] JACQUET P. et al., Physics of Plasmas 21 (2014) pp.061510
[8] BOBKOV V. et al., Journal of Nucl. Materials 438 (2013) S160–S165,
[9] PÜTTERICH T., IAEA FEC2012, San Diego, EX/P3–15 (2012),
[10] VAN EESTER D. et al., Proc. 41st EPS Conf. Plasma Physics, Berlin, June 2014,
[11] LERCHE E. et al., Nucl. Fusion 56 (2016) 036022 (19pp)
[12] DEN HARDER N. et al., Nucl. Fusion 56 (2016) 026014 (9pp)
[13] COLAS L. et al. Nucl. Fusion 46 (2006) S500–S513
[14] JACQUET P. et al., Journal of Nuc. Materials 438 (2013) S379–S383
[15] NUNES I. et al., Plasma Physics and Control. Fusion 58 (2016) 014034 (10 pp.)
[16] PÜTTERICH T. et al., Plasma Phys. Control. Fusion 55 (2013) 124036 (11pp)
[17] CHALLIS C. et al., Nucl. Fusion 55 (2015) 053031 (18pp),
[18] ANGIONI C. et al., Plasma Phys. Control. Fusion 51 (2009) 124017 (14pp)